

Test of the Brink-Axel Hypothesis for the Pygmy Dipole Resonance

D. Martin,¹ P. von Neumann-Cosel,^{1,*} A. Tamii,² N. Aoi,² S. Bassauer,¹ C. A. Bertulani,³ J. Carter,⁴ L. Donaldson,⁴ H. Fujita,² Y. Fujita,² T. Hashimoto,² K. Hatanaka,² T. Ito,² A. Krugmann,¹ B. Liu,² Y. Maeda,⁵ K. Miki,² R. Neveling,⁶ N. Pietralla,¹ I. Poltoratska,¹ V. Yu. Ponomarev,¹ A. Richter,¹ T. Shima,² T. Yamamoto,² and M. Zweidinger¹

¹*Institut für Kernphysik, Technische Universität Darmstadt, D-64289 Darmstadt, Germany*

²*Research Center for Nuclear Physics, Osaka University, Ibaraki, Osaka 567-0047, Japan*

³*Department of Physics and Astronomy, Texas A&M University-Commerce, Commerce, Texas 75429, USA*

⁴*University of the Witwatersrand, Johannesburg 2050, South Africa*

⁵*Faculty of Engineering, Miyazaki University, Miyazaki 889-2192, Japan*

⁶*iThemba LABS, Somerset West 7129, South Africa*

(Dated: November 8, 2016)

The gamma strength function (GSF) and level density (LD) of 1^- states in ^{96}Mo have been extracted from a high-resolution study of the (p, p') reaction at 295 MeV and extreme forward angles. The GSF agrees with results of compound nucleus γ decay experiments in the energy region of the Pygmy Dipole Resonance (PDR), validating the generalized Brink-Axel hypothesis commonly assumed in astrophysical reaction network calculations. The consistency of the LD deduced from the present data with those of the γ decay experiments provides independent confirmation of the methods used to separate GSF and LD in Oslo-type experiments.

Introduction.—Gamma Strength Functions describe the average γ decay behavior of a nucleus as a function of excitation energy. Their knowledge is required for applications of statistical nuclear theory in astrophysics [1], reactor design [2], and waste transmutation [3]. Although all electromagnetic multipoles contribute, the GSF is dominated by the E1 radiation with smaller contributions from M1 strength. Above particle threshold it is governed by the IsoVector Giant Dipole Resonance (IVGDR) but at lower excitation energies the situation is complex: In nuclei with neutron excess one observes the formation of the Pygmy Dipole Resonance (PDR) [4] sitting on the low-energy tail of the IVGDR. The impact of low-energy E1 strength on astrophysical reaction rates and the resulting abundances in the r process have been discussed e.g. in Refs. [5–7].

Most applications imply an environment of finite temperature, notably in stellar scenarios [8], and thus reactions on initially excited states become relevant. Their contributions to the reaction rates are usually estimated applying the generalized Brink-Axel (BA) hypothesis [9, 10], which states that the GSF is independent of the properties of the initial and final states and thus should be the same in γ emission and absorption experiments. Although historically formulated for the IVGDR, where it seems to hold approximately for not too high temperatures [11], this is nowadays a commonly used assumption to calculate the low-energy E1 and M1 strength functions. However, a recent shell-model analysis [12] puts that into question. It demonstrates that the strength functions of collective modes built on excited states do show an energy dependence and this is expected from spectral distribution theory. The numerical results for E1 strength functions, however, showed an approximate constancy as a function of excitation energy consistent

with the BA hypothesis.

Recent work utilizing compound nucleus γ decay with the so-called Oslo method [13] has demonstrated independence of the GSF from excitation energies and spins of initial and final states in a given nucleus in accordance with the BA hypothesis once the level densities are sufficiently high to suppress large intensity fluctuations [14]. However, there are a number of experimental results which indicate violations of the BA hypothesis in the low-energy region. For example, the GSF in heavy deformed nuclei at excitation energies of 2 – 3 MeV is dominated by the orbital M1 scissors mode [15] and potentially large differences in $B(\text{M1})$ strengths are observed between γ emission and absorption experiments [16–18]. At very low energies (< 2 MeV) an increase of GSFs is observed in Oslo-type experiments [19, 20], which for even-even nuclei cannot have a counterpart in ground state absorption experiments because of the pairing gap.

For the low-energy E1 strength in the region of the PDR, the question is far from clear when comparing results from the Oslo method with photoabsorption data. Below particle thresholds most information on the GSF stems from nuclear resonance fluorescence (NRF) experiments. A striking example of disagreement is the GSF of ^{96}Mo , where the results from the Oslo method [21, 22] and from NRF [23] differ by factors 2 – 3 at excitation energies between 4 and 7 MeV. A problem with the NRF method are the experimentally unobserved branching ratios to excited states. While many older analyses of NRF data assume that these are negligible, in Ref. [23] they are included by a Hauser-Feshbach calculation assuming statistical decay. The resulting corrections are sizable, reaching a factor of five close to the neutron threshold. On the other hand, there are indications of non-statistical decay behavior of the PDR from recent measurements

[24, 25]. Violation of the BA hypothesis was also claimed in a simultaneous study of the (γ, γ') reaction and average ground state branching ratios [26] in ^{142}Nd (see, however, Ref. [27]). Clearly, information on the GSF – in particular in the energy region of the PDR – from an independent experiment is called for.

A new method for the measurement of complete E1 strength distributions – and thereby the E1 part of the GSFs – in nuclei from about 5 to 25 MeV has been developed using relativistic Coulomb excitation in polarized inelastic proton scattering at energies of a few hundred MeV and scattering angles close to 0° [28–31]. These data allow the dipole polarizability to be determined which provides important constraints on the neutron skin of nuclei and the poorly known parameters of the symmetry energy [32]. They also allow extraction of the M1 part of the GSF due to spinflip excitations [33], which energetically overlaps with the PDR strength. Here, a study of ^{96}Mo is reported aiming at a critical examination of the apparent violation of the BA hypothesis in the low-energy regime suggested by the NRF data.

Experiment.—The $^{96}\text{Mo}(\vec{p}, \vec{p}')$ reaction was studied at RCNP, Osaka, Japan. Details of the experimental techniques can be found in Ref. [34]. A proton beam of 295 MeV with intensities of about 2 nA at 0° up to 6 nA at larger spectrometer angles and with an average polarization $P_0 \simeq 0.67$ impinged on a ^{96}Mo foil isotopically enriched to 96.7% with an areal density of 3 mg/cm². Data were taken with the Grand Raiden spectrometer [35] placed at 0° covering an angular acceptance of $\pm 2.6^\circ$ and excitation energies $E_x \simeq 5$ –23 MeV. The energy resolution varied between 25 and 40 keV (full width at half maximum, FWHM). Normally (N) and longitudinally (L) polarized beams were used to measure the polarization transfer coefficients [36] $D_{NN'}$ and $D_{LL'}$, respectively. Additional data with unpolarized protons were taken for angles up to 6° .

Figure 1(a) displays the spectra taken at spectrometer angles 0° , 3° , and 4.5° . Besides discrete transitions at low excitation energies, a resonance-like structure around 8 MeV and the prominent IVGDR centered at $E_x \approx 16$ MeV are observed. The cross sections show a strong forward-angle peaking indicating the dominance of Coulomb excitation. The total spin transfer

$$\Sigma = \frac{3 - (2D_{NN'} + D_{LL'})}{4} \quad (1)$$

shown in Fig. 1(b) can be extracted from the measured polarization transfer observables. It takes a value of one for spinflip ($\Delta S = 1$) and zero for non-spinflip ($\Delta S = 0$) transitions at 0° [37], interpreted as M1 and E1 cross sections parts, respectively. Values in between 0 and 1 result from the summation over finite energy bins (200 keV up to an excitation energy of 10 MeV and 500 keV above). The polarization transfer analysis (PTA) reveals a concentration of spinflip strength in the energy region

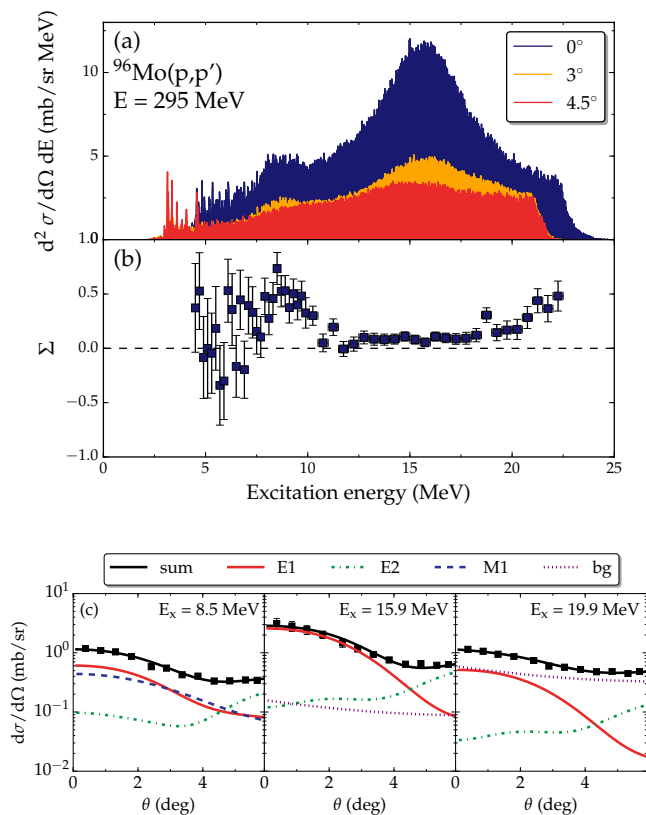


FIG. 1. (Color online) (a) Spectra of the $^{96}\text{Mo}(\vec{p}, \vec{p}')$ reaction at $E_p = 295$ MeV with the spectrometer placed at 0° (blue), 3° (yellow), and 4.5° (red). (b) Total spin transfer Σ , Eq. (1). (c) Examples of the MDA for selected energy bins.

7.5–10 MeV identified as the spin-M1 resonance in ^{96}Mo while cross sections above 10 MeV are dominantly of $\Delta S = 0$ character as expected for Coulomb excitation. These findings are consistent with the results in ^{208}Pb [28] and ^{120}Sn [31]. The $\Delta S = 1$ strength observed at high E_x can be understood to arise from quasi-free scattering [38].

Alternatively, a multipole decomposition analysis (MDA) was performed for angular distributions of the cross sections in the PDR and GDR regions. For this purpose, angular cuts were applied to the spectra of Fig. 1(a) providing 4 data points each. The MDA followed closely the approach described in Refs. [28, 29]. For the nuclear background the empirical parametrization found for ^{208}Pb [39] was adopted assuming the same momentum transfer dependence. Figure 1(c) presents representative examples of the MDA for 200 keV excitation energy bins at different excitation energies. They demonstrate that in the low-energy bump M1 contributions are sizable while E1 dominates in the energy region of the IVGDR. At even higher energies, the nuclear background becomes relevant. Spinflip and non-spinflip cross sections from the MDA and PTA for $E_x \leq 11$ MeV are compared in Fig. 2. The two completely independent decomposition

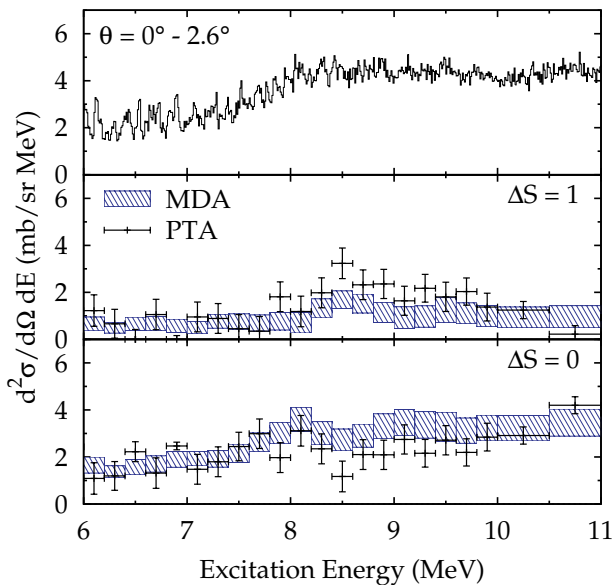


FIG. 2. (Color online) Decomposition of non-spinflip ($\Delta S = 0$) and spinflip ($\Delta S = 1$) cross section parts in the $^{96}\text{Mo}(\bar{p}, \bar{p}')$ reaction in the excitation energy region 6 – 11 MeV based on the MDA and PTA, respectively. Good agreement between the two independent methods is observed.

methods lead to consistent results within error bars except for one energy bin around 8.5 MeV. In the following, E1 and M1 cross sections averaged over both decomposition methods are considered for excitation energies up to 11 MeV. At higher E_x the MDA results are taken since the $\Delta S = 0$ part of the nuclear background, which cannot be distinguished in the PTA, becomes relevant.

Gamma Strength Function.—The GSF for electric or magnetic transitions $X \in \{E, M\}$ with multipolarity λ is related to the photoabsorption cross section $\langle \sigma_{abs}^{X\lambda} \rangle$ by

$$f^{X\lambda}(E, J) = \frac{2J_0 + 1}{(\pi \hbar c)^2 (2J + 1) E^{2\lambda - 1}} \langle \sigma_{abs}^{X\lambda} \rangle, \quad (2)$$

where E denotes the γ energy and J, J_0 are the spins of excited and ground state, respectively [40]. The brackets $\langle \rangle$ indicate averaging over an energy interval. In practice only E1 and M1 transitions provide sizable contributions to the total GSF. The Coulomb excitation cross sections representing the E1 part of the GSF were converted to equivalent photoabsorption cross sections using the virtual photon method [41]. The virtual photon spectrum was calculated in an eikonal approach [42] and integrated over the solid angle covered by the experiment. The M1 cross sections from Fig. 2 were converted to reduced transition strengths and the corresponding M1 photoabsorption cross sections with the approach described in Ref. [33].

The sum approximating the total GSF in ^{96}Mo is displayed in Fig. 3(a) as red circles for excitation energies $E_x = 5 - 22$ MeV. The result is compared with

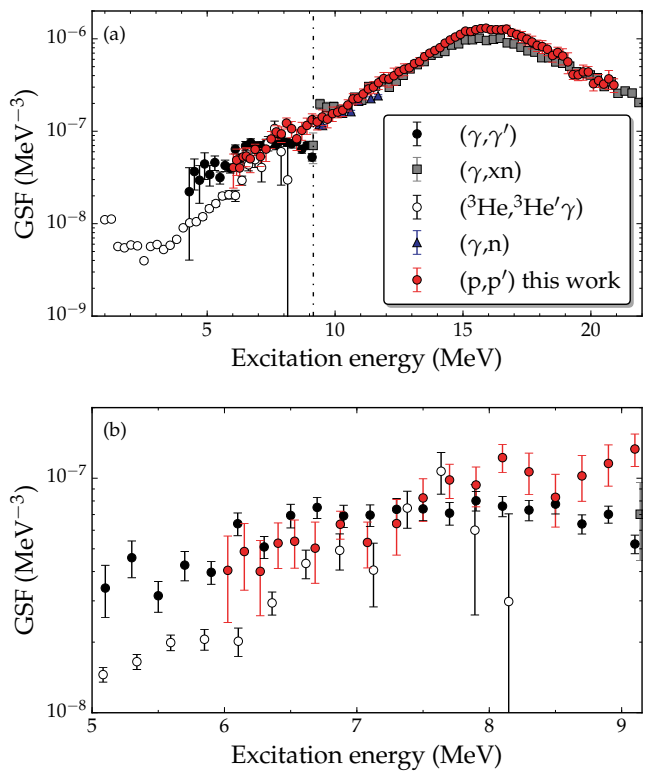


FIG. 3. (Color online). (a) GSF of ^{96}Mo from the present work (red circles) compared with $(^3\text{He}, ^3\text{He}'\gamma)$ [21, 22] (open circles), (γ, xn) [43] (grey squares), (γ, n) [44], (blue upward triangles) and (γ, γ') [23] data including a statistical model correction for unobserved branching ratios (black circles) (b) Expanded range from 5 MeV to neutron threshold.

$(^3\text{He}, ^3\text{He}'\gamma)$ [21, 22] (open circles), (γ, xn) [43] (grey squares), (γ, n) [44] (blue upward triangles), and (γ, γ') data corrected for unobserved branching ratios [23] (black circles). Above threshold, there is overall fair agreement with the data from Refs. [43, 44] except that the present experiment finds somewhat larger photoabsorption cross sections around the maximum of the IVGDR.

Below S_n , the GSF from the present work lies in between the Oslo and the (γ, γ') experiment. An expanded view of the GSF results between 5 MeV and the neutron threshold $S_n = 9.154$ MeV is displayed in Fig. 3(b). The (p, p') and $(^3\text{He}, ^3\text{He}'\gamma)$ results agree within error bars except for the two lowest excitation energies analyzed in the present data. However, these two data points suffer from limited statistics. The (γ, γ') results [23] agree in the 7 – 8 MeV excitation energy region 7 – 8 MeV but clearly underestimate the present results at higher E_x . At lower E_x they are systematically at the upper limit of the present results (and sometimes exceed it) and are significantly larger than the Oslo results. The deviations from the present results may arise from the modeling of the large atomic background in the spectra and/or the specific choice of level densities for the simulation of the

γ decay cascades [45].

Level Density.—Since by the Oslo method only the product of GSF and LD is measured [13] and it thus relies on external data for their decomposition, an independent check of the LD results for ^{96}Mo is of high importance. The good energy resolution of the present data of about 25 keV full width at half maximum permits an extraction of the $J^\pi = 1^-$ LD in the energy region of the IVGDR applying a fluctuation analysis. Details of the method can be found in Refs. [46–48]. In order to compare with the Oslo results, the 1^- LD values are converted to a total level density using the backshifted Fermi gas (BSFG) model [49] and assuming parity equilibration [50]. Since the spin distribution depends on the chosen BSFG parameters, one needs to consider the model dependence of the procedure. It is taken into account by averaging over results from three BSFG parameter sets [40, 51, 52] and taking their variance as a measure of the model uncertainty.

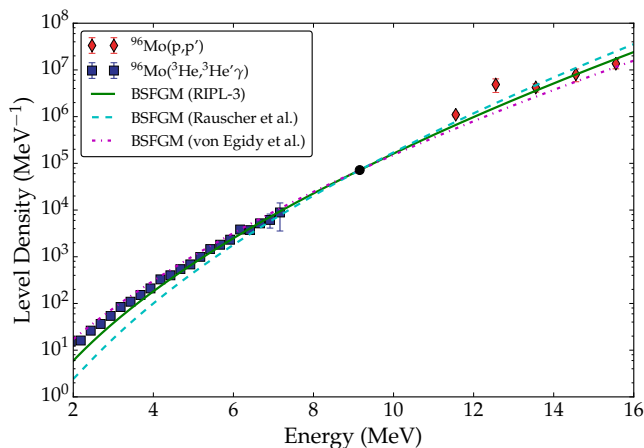


FIG. 4. (Color online). Total LD in ^{96}Mo deduced from the fine structure of the (p, p') data in the energy region of the IVGDR (red diamonds) compared with the results from the $(^3\text{He}, ^3\text{He}'\gamma)$ Oslo experiment (blue squares) [21, 22]. The black circle point stems from s -wave resonance neutron capture [44]. BSFG models normalized to the value at S_n are shown as green solid [40], cyan dashed [51], and purple dashed-dotted [52] lines.

The LD obtained between 11.5 and 15.5 MeV (red diamonds) is presented in Fig. 4 together with the Oslo results at lower excitation energies (blue squares) and s -wave neutron capture (black circle) [44]. The BSFG models normalized to the value at S_n are displayed as green solid [40], cyan dashed [51], and purple dashed-dotted [52] lines, respectively. In particular, the BSFG parameters from the systematics of RIPL-3 [40] provide a satisfactory description of all data over a large excitation energy range, consistent with a similar analysis for ^{208}Pb [49].

Conclusions.—The gamma strength function of ^{96}Mo has been extracted from a study of the (p, p') reaction at

295 MeV and extreme forward angles. The GSF agrees with results of compound nucleus γ decay experiments indicating that the BA hypothesis holds in the energy region of the PDR, in contrast to results from the (γ, γ') reaction [23] and the claims of Ref. [26]. This is an important finding since the BA hypothesis constitutes a general presupposition for astrophysical reaction network calculations. The high energy resolution and selectivity of the data permits an extraction of the LD at excitation energies above the neutron threshold hardly accessible by other means. A consistent description of the LD with those of the γ decay experiments can be achieved within BSFG models providing independent confirmation of the methods used to separate GSF and LD in Oslo-type experiments.

While the present results support a use of the BA hypothesis for statistical model calculations of reaction cross sections in finite temperature environments, a general statement requires a systematic comparison of GSFs derived from γ absorption and emission experiments in the energy range of the PDR over a broad range of nuclei. For example, the role of deformation needs to be explored by comparing spherical and well-deformed cases with the present results for the moderately deformed ^{96}Mo . Work along these lines is under way.

We are indebted to the RCNP for providing excellent beams. Discussions with M. Guttormsen, E. Grosse, A. C. Larsen, R. Schwengner, and S. Siem are gratefully acknowledged. This work has been supported by the DFG under contract SFB 1245 and by MEXT KAKENHI Grant Number JP25105509. C.A.B. acknowledges support by the U.S. DOE grant DE-FG02-08ER41533 and the U.S. NSF Grant No. 1415656.

* E-mail: vnc@ikp.tu-darmstadt.de

- [1] M. Arnould, S. Goriely, and K. Takahashi, *Phys. Rep.* **450**, 97 (2007).
- [2] M. B. Chadwick *et al.*, *Nucl. Data Sheets* **112**, 2887 (2011).
- [3] M. Salvatore and G. Palmiotti, *Prog. Part. Nucl. Phys.* **66**, 144 (2011).
- [4] D. Savran, T. Aumann, and A. Zilges, *Prog. Part. Nucl. Phys.* **70**, 210 (2013).
- [5] S. Goriely, E. Khan, and M. Samyn, *Nucl. Phys.* **A739**, 331 (2004).
- [6] E. Litvinova, H. P. Loens, K. Langanke, G. Martínez-Pinedo, T. Rauscher, P. Ring, F.-K. Thielemann, and V. Tselyaev, *Nucl. Phys.* **A823**, 26 (2009).
- [7] I. Daoutidis and S. Goriely, *Phys. Rev. C* **86**, 034328 (2012).
- [8] M. Wiescher, F. Käppeler, and K. Langanke, *Annu. Rev. Astron. Astrophys.* **50**, 165 (2012).
- [9] D. M. Brink, Ph.D. thesis, Oxford University (1955).
- [10] P. Axel, *Phys. Rev.* **126**, 671 (1962).
- [11] P. F. Bortignon, A. Bracco, and R. A. Broglia, *Giant Resonances: Nuclear Structure at Finite Temperature* (Har-

- wood Academic, Amsterdam, 1998).
- [12] C. W. Johnson, Phys. Lett. B **750**, 72 (2015).
- [13] A. Schiller, L. Bergholt, M. Guttormsen, E. Melby, J. Rekstad, and S. Siem, Nucl. Instrum. Methods Phys. Res., Sect. A **447**, 498 (2000).
- [14] M. Guttormsen, A. C. Larsen, A. Görden, T. Renstrom, S. Siem, T. G. Tornyi, and G. M. Tveten, Phys. Rev. Lett. **116**, 012502 (2016).
- [15] D. Bohle, A. Richter, W. Steffen, A. E. L. Dieperink, N. Lo Iudice, F. Palumbo, and O. Scholten, Phys. Lett. B **137**, 27 (1984).
- [16] K. Heyde, P. von Neumann-Cosel, and A. Richter, Rev. Mod. Phys. **82**, 2365 (2010).
- [17] M. Guttormsen *et al.*, Phys. Rev. Lett. **109**, 162503 (2012).
- [18] C. T. Angell, R. Hajima, and T. Shizuma, B. Ludewigt and B. J. Quiter, Phys. Rev. Lett. **117**, 142501 (2016).
- [19] A. Voinov, E. Algin, U. Agvaanluvsan, T. Belgya, R. Chankova, M. Guttormsen, G. E. Mitchell, J. Rekstad, A. Schiller, and S. Siem, Phys. Rev. Lett. **93**, 142504 (2004).
- [20] A. C. Larsen *et al.*, EPJ Web of Conferences **66**, 07014 (2014).
- [21] M. Guttormsen *et al.*, Phys. Rev. C **71**, 044307 (2005).
- [22] A. C. Larsen and S. Goriely, Phys. Rev. C **82**, 014318 (2010).
- [23] G. Rusev *et al.*, Phys. Rev. C **79**, 061302 (2009).
- [24] C. Romig *et al.*, Phys. Lett. B **744**, 369 (2015).
- [25] B. Löher *et al.*, Phys. Lett. B **756**, 72 (2016).
- [26] C. T. Angell, S. L. Hammond, H. J. Karwowski, J. H. Kelley, M. Krtička, E. Kwan, A. Makinaga, and G. Rusev, Phys. Rev. C **86**, 051302(R) (2012).
- [27] Erratum to Ref. [27], Phys. Rev. C **91**, 039901(E) (2015).
- [28] A. Tamii *et al.*, Phys. Rev. Lett. **107**, 062502 (2011).
- [29] I. Poltoratska *et al.*, Phys. Rev. C **85**, 041304(R) (2012).
- [30] A. M. Krumbholz *et al.*, Phys. Lett. B **744**, 7 (2015).
- [31] T. Hashimoto *et al.*, Phys. Rev. C **92**, 031305(R) (2015).
- [32] *Topical Issue on Nuclear Symmetry Energy*, edited by Bao-An Li, A. Ramos, G. Verde and I. Vidaña, Eur. Phys. J. A **50**(2), (2014).
- [33] J. Birkhan, H. Matsubara, P. von Neumann-Cosel, N. Pietralla, V. Yu. Ponomarev, A. Richter, A. Tamii, and J. Wambach, Phys. Rev. C **93**, 041302(R) (2016).
- [34] A. Tamii *et al.*, Nucl. Instrum. Methods Phys. Res., Sect. A **605**, 3 (2009).
- [35] M. Fujiwara *et al.*, Nucl. Instrum. Methods Phys. Res., Sect. A **422**, 488 (1999).
- [36] G. G. Ohlsen, Rep. Prog. Phys. **35**, 717 (1979).
- [37] T. Suzuki, Prog. Theor. Phys. **321**, 859 (2000).
- [38] F. T. Baker *et al.*, Phys. Rep. **289**, 235 (1997).
- [39] I. Poltoratska, Doctoral thesis D17, TU Darmstadt (2011); [<http://tuprints.ulb.tu-darmstadt.de/2671>].
- [40] R. Capote *et al.*, Nucl. Data Sheets **110**, 3107 (2009).
- [41] C. A. Bertulani and G. Baur, Phys. Rep. **163**, 299 (1988).
- [42] C. A. Bertulani and A. M. Nathan, Nucl. Phys. **A554**, 158 (1993).
- [43] H. Beil, R. Bergère, P. Carlos, A. Leprêtre, A. De Miniac, and A. Veyssiere, Nucl. Phys. **A227**, 427 (1974).
- [44] H. Utsunomiya *et al.*, Phys. Rev. C **88**, 015805 (2013).
- [45] G. Rusev *et al.*, Phys. Rev. C **77**, 064321 (2008).
- [46] Y. Kalmykov *et al.*, Phys. Rev. Lett. **96**, 012502 (2006).
- [47] I. Usman *et al.*, Phys. Rev. C **84**, 054322 (2011).
- [48] I. Poltoratska, R. W. Fearick, A. M. Krumbholz, E. Litvinova, H. Matsubara, P. von Neumann-Cosel, V. Yu. Ponomarev, A. Richter, and A. Tamii, Phys. Rev. C **89**, 054322 (2014).
- [49] S. Bassauer, P. von Neumann-Cosel, and A. Tamii, Phys. Rev. C (in press); arXiv1609.0937.
- [50] Y. Kalmykov, C. Özen, K. Langanke, G. Martínez-Pinedo, P. von Neumann-Cosel, and A. Richter, Phys. Rev. Lett. **99**, 202502 (2007).
- [51] T. Rauscher, F.-K. Thielemann, and K.-L. Kratz, Phys. Rev. C **56**, 1613 (1997).
- [52] T. von Egidy and D. Bucurescu, Phys. Rev. C **72**, 044311 (2005).